Available online at www.sciencedirect.com
ScienceDirect
Journal of Nuclear Materials 375 (2008) 315–322
journal of nuclear materials
www.elsevier.com/locate/jnucmat

Stainless steel/glass–ceramic interactions under hot isostatic pressing (HIPing) conditions

Y. Zhang *, H. Li, P.J. McGlinn, B. Yang, B.D. Begg

Australian Nuclear Science & Technology Organisation, PMB 1, Menai, NSW 2234, Australia

Received 30 May 2006; accepted 30 October 2007

Abstract

The interactions between stainless steel (SS) and a glass–ceramic designed for immobilisation of the high-level nuclear waste generated at the Idaho chemical processing plant (ICPP) under hot isostatic pressing (HIPing) conditions (100 MPa in argon at 1200 °C) have been studied and subsequently the effect of such interactions on the chemical durability of the glass–ceramic waste form has been examined. The diffusion of Cr from SS (Cr depletion in SS) through the interaction layer and formation of crystalline Cr/Al oxides in glass dominate the overall interaction process. It appears that the depletion of Cr in SS may reduce the potential of SS as a barrier. However, such interactions have no significant impact on the glass–ceramic and the presence of the interaction layer does not seem to have any detrimental effect on the chemical durability of the glass–ceramic as a waste form.

1. Introduction

High-level radioactive waste (HLW) generated at the Idaho chemical processing plant (ICPP) from the reprocessing of irradiated defense nuclear fuel is currently stored at the Idaho National Laboratory (INL) in a calcined form [1]. Although there are several types of HLW Idaho calcines, the majority of the calcine consists of ~50 wt% of CaF_2 and ~50 wt% of metal oxides such as $A1_2O_3$, ZrO_2 and B_2O_3. Radionuclide content is generally <1 wt% and the radionuclides are typical for products of ^{235}U fission [1].

The calcined waste is temporarily stored in near surface impoundments in SS bins within concrete vaults. However, it may have to be immobilised in a suitable waste form before being sent to a Federal repository. Typical glass waste forms would result in large volumes of immobilized waste due to their relatively low waste loadings (~30 wt%) for the calcined waste. A tailored glass–ceramic waste form was therefore developed at ANSTO as a cost-saving alternative by increasing the waste loading to ~80 wt%, achieving ~25% greater density and ~65% less immobilised waste volume than a glass waste form [2,3].

Hot isostatic pressing (HIPing) was selected by ANSTO for the production of the glass–ceramic, because of its flexible processing environment and extremely low off-gas emissions due to the calcine and precursor components being sealed in SS cans prior to the hot consolidation step. We studied the SS/glass interactions under HIPing conditions to understand whether such metal/glass interactions would have any detrimental effect on the waste form long-term stability. In this paper, we report the microscopic characterisation of the SS/glass interactions under HIPing conditions and the effect of such interactions on the chemical durability of the glass–ceramic waste form.

2. Experimental

Glass–ceramic samples (measuring approximately 2.5 cm in diameter and 2 cm high and weighing about 30 g each) were prepared by a typical oxide route with 80% of simulated calcined waste [2] and HIPed at 1200 °C for 2 h under 100 MPa pressure in an argon atmosphere. They are low Na (Na_2O ~2 wt%) borosilicate based glass–ceramics containing ~0.3 wt% of Cr_2O_3 and ~0.6 wt% of Fe_2O_3,

* Corresponding author. Tel.: +61 2 9717 9156; fax: +61 2 9543 7179.
E-mail address: yzx@ansto.gov.au (Y. Zhang).

0022-3115/$ - see front matter © 2008 Elsevier B.V. All rights reserved.
doi:10.1016/j.jnucmat.2007.10.018

respectively, in glass. The HIP can was 1 mm thick 304 grade SS.

The sample for characterisation by scanning electron microscopy (SEM) was cut from the glass–ceramic adjacent to the SS can, cross-sectionally mounted in epoxy resin, and polished to a 0.25 μm diamond finish. SEM was carried out with a JEOL JSM-6300 instrument operated at 15 kV, and fitted with a NORAN Voyager IV X-ray microanalysis system (EDX). Calibrations for microanalysis were carried out using a comprehensive set of standards for quantitative analysis [4]. X-ray diffraction was carried out on a Panalytical X'Pert Pro diffractometer using Ni filtered Cu Kα radiation ($\lambda = 0.15418$ nm) with an X'cellerator multichannel detector utilising a real time multiple strip technology.

One of the samples was used for durability testing as a whole HIPed specimen with the can-waste form interaction layer essentially intact (HIPed can was carefully removed). A number of smaller, tabular sub-specimens measuring $8 \times 8 \times 2$ mm in size were prepared for parallel durability tests. These tabular sub-specimens had the outer SS can-waste form interaction layer cut off during preparation, specifically to determine whether the presence of such interaction layer has any effect on the durability of the waste form. They were characterised before and after leaching by SEM to examine micro-textural changes on the surfaces. In addition, cross-section samples were also prepared to enable determination of the depth of alteration of the specimen, as a result of leaching. The tabular sub-specimens prepared from the HIPed material were cut and coarsely ground, to remove cutting saw marks, for durability testing. The surfaces of the sub-specimens were not polished in this instance so that the surfaces would approximate the textural finish of the surface of the whole HIPed sample. This was carried out to minimise any differences in surface area measurements brought about by differences in surface texture/ roughness, which in turn would affect normalised release rate calculations. Fig. 1 shows a SS can before and after HIPing (1(a) and (b)), a whole HIPed specimen 1(c) and a tabular sub-specimen 1(d).

To elucidate the effect of SS/glass–ceramic interactions on the overall chemical durability of the waste form, the whole HIPed specimen and the tabular sub-specimens were leached singly and in duplicate, respectively, in deionised water at 90 °C for 56 days, using a modified version of the ASTM standard for static leaching of monolithic waste forms [5]. The leachates were completely replaced with fresh deionised water at the end of each time interval (1, 7, 14 and 35 days) to avoid steady-state conditions being reached. Each leachate, including that for the final leach period (35–56 days), was analysed using ICP-MS for cations and an ion selective electrode (ISE) for fluorine releases.

In order to determine leach rates, surface area measurements were made of the specimens. For the tabular sub-specimens this was straightforward measurement using an RS digital electronic micrometer, based on the linear dimensions of the sub-specimens. The whole HIPed specimens had irregular surfaces and surface area measurement in this case was carried out using 3D laser technology. Scanning the surface of the specimens was carried out using a Konica Minolta Vivid 9i laser scanner fitted with a telephoto lens with a 0.1 mm resolution and accuracy of ±0.05 mm. Measurements of the scans were taken using Rhino 3D v3.0 software and data processing completed in Raindrop Geomagic Studio v7 to provide surface area determinations.

3. Results and discussion

3.1. Characterisation of the glass–ceramic

A SEM backscattered electron micrograph of the bulk of the HIPed glass–ceramic is shown in Fig. 2. Two crystalline phases, zirconia (ZrO_2) and fluorite (CaF_2) are randomly distributed in an amorphous, chemically uniform borosilicate glass matrix [2].

3.2. Characterisation of the outer surface of the SS HIPed can

Fig. 3 shows the cross-sectional SEM backscattered electron micrograph of the outer surface of the HIPed can. A thin oxide layer (up to 3 μm in thickness), formed on the

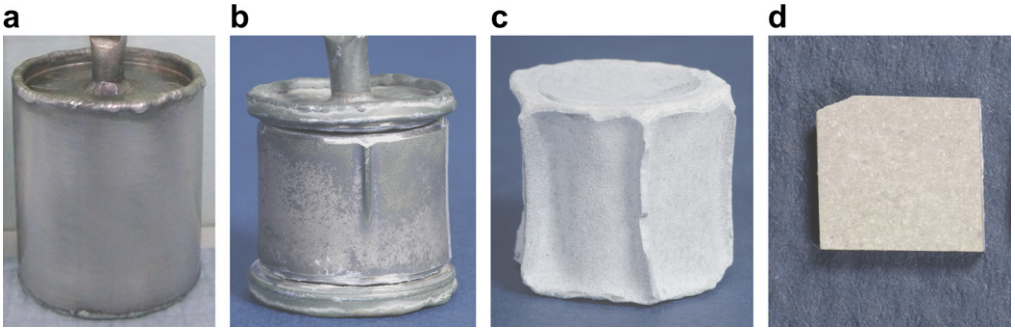

Fig. 1. Shapes and configurations of (a) a SS can before HIPing; (b) a SS can after HIPing; (c) a whole HIPed specimen after peeling off the SS can and (d) a tabular sub-specimen ($8 \times 8 \times 2$ mm) cut off from the middle of the whole HIPed specimen.

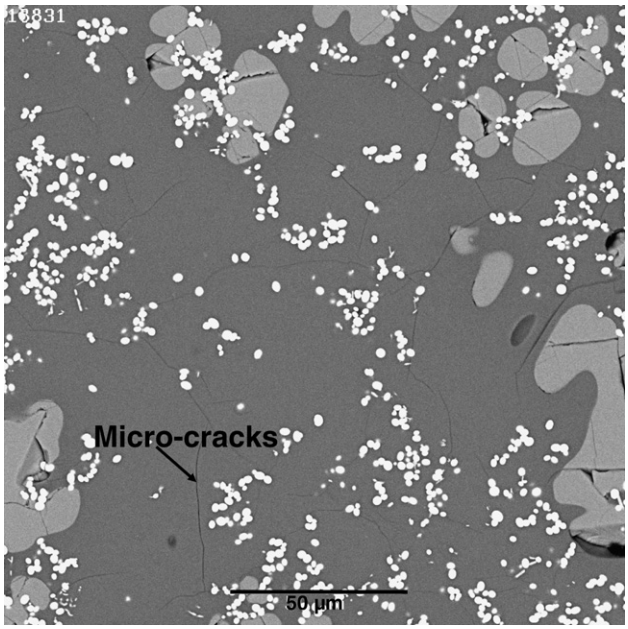

Fig. 2. SEM backscattered electron micrograph of the matrix of the HIPed glass–ceramic (zirconia – small bright rounded particles; fluorite – large grey irregular dendritic forms; and glass – dark grey background).

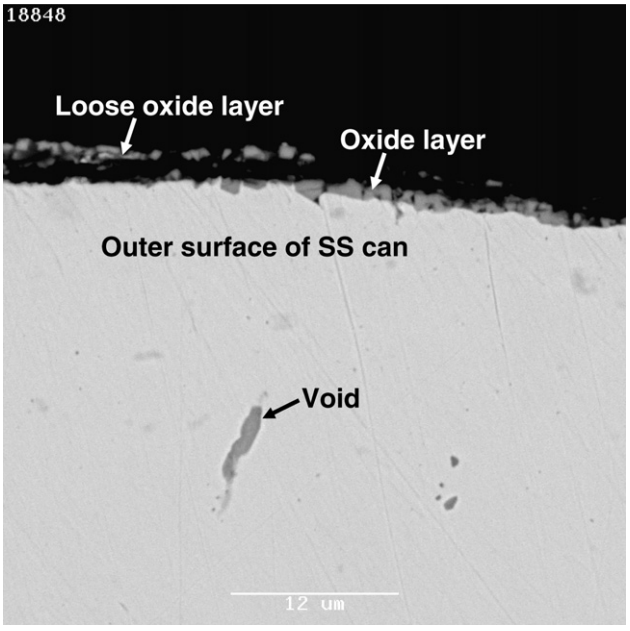

Fig. 3. Cross-sectional SEM backscattered electron micrograph of the outer surface of the SS can after HIPing showing the formation of an oxide layer up to 3 μm thick.

outer surface of the can, contains Cr/Fe oxides. Cr and Mn depletions in the SS adjacent to the oxide layer were also detected (see Table 1). These results are consistent with the presence of $\leqslant$10 ppm O_2 in the industry pure argon gas being used for HIPing.

The X-ray diffraction patterns with the corresponding indices for the outside of the SS can after and before HIPing are shown in Fig. 4(a) and (b), respectively. For the SS

Table 1
Elemental profiles (wt%) of the SS immediately adjacent to the oxide layer on the outer surface of the HIPed can

Depth[a] (μm)	Fe	Cr	Ni	Mn
1	72.5	17.8	8.5	0.5
10	69.9	19.4	8.4	1.4
20	69.0	19.4	8.9	1.8
30	69.8	19.5	8.2	1.7

[a] Proceeding inwards from oxide layer.

before HIPing, five peaks are present in the diffraction pattern (b), consistent with the published X-ray diffraction data for 304 SS [6]. For the SS after HIPing (see pattern in Fig. 4(a)), the diffraction peaks are due to Fe_3O_4, Cr_2O_3, ferrite and the SS. Fe_3O_4 forms a cubic phase with lattice parameter $a = 0.8426$ (6) nm which is about 0.3% larger than that reported earlier [7], probably because of substitution of impurities in the Fe_3O_4 formed here.

The sectioned SEM sample was then etched and characterised by using an optical microscope. The optical micrograph (see Fig. 5) indicated that a thin layer of ferrite phase was formed immediately under the oxide layer on the outer surface of the SS can due to the Cr depletion, which is consistent with XRD results.

3.3. Characterisation of the reaction interface between the SS and the glass–ceramic

The SEM backscattered electron micrograph of the interface between the SS can and the glass–ceramic is shown in Fig. 6. The gap between the SS and the glass–ceramic is the result of sample preparation (cutting and mounting) implying low adhesion at the interface. There does not seem to be any obvious microstructural variation in the glass–ceramic near the interface, although the reaction has resulted in subtle chemical composition changes, as determined by EDS, in both the SS and the glass (see below). There were no detectable changes in the composition of the two crystalline ceramic phases, zirconia and fluorite.

Fig. 7 shows the SEM backscattered electron micrograph of the SS component of the can–waste form interface and the profiles of Fe, Cr and Ni concentrations from the interface into the can. The Cr depletion (and Fe enrichment) layer is around 40 μm thick whilst Ni remains essentially constant. In a few cases, some glass fragments have penetrated into the SS matrix via grain boundaries due to the high pressure and temperature to which the SS grain boundaries were subjected.

SEM observations of the glass matrix revealed the formation of a band of an acicular phase at 200–400 μm below the interface (see Fig. 8). EDS analysis confirmed that the phase is a mixture of Cr and Al oxides with molar ratio approximately 3 to 1. The phase diagram of Cr_2O_3 and Al_2O_3 [8] suggests that they can form a continuous solid solution due to their similar crystal structures. The

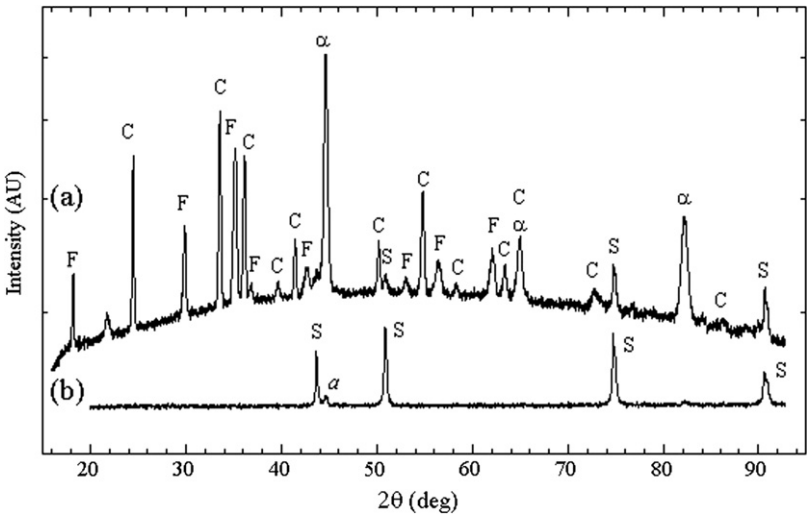

Fig. 4. X-ray diffraction patterns for the SS after (a) and before (b) HIPing with the corresponding indices (S-SS, α-ferrite, C-Cr_2O_3 and F-Fe_3O_4).

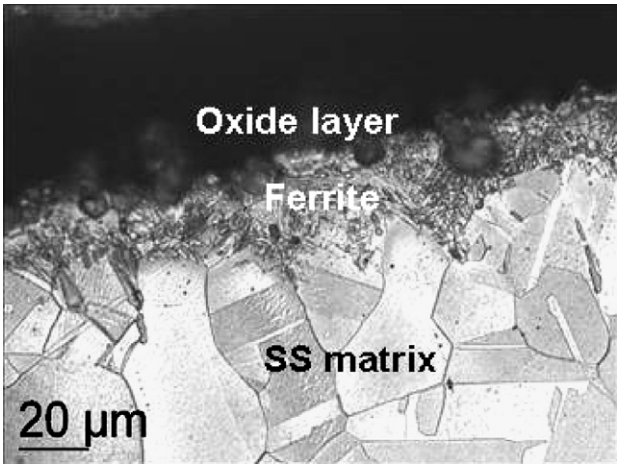

Fig. 5. Optical micrograph of the SEM sample after etching shows the presence of ferrite immediately under the oxide layer on the outside of the SS can.

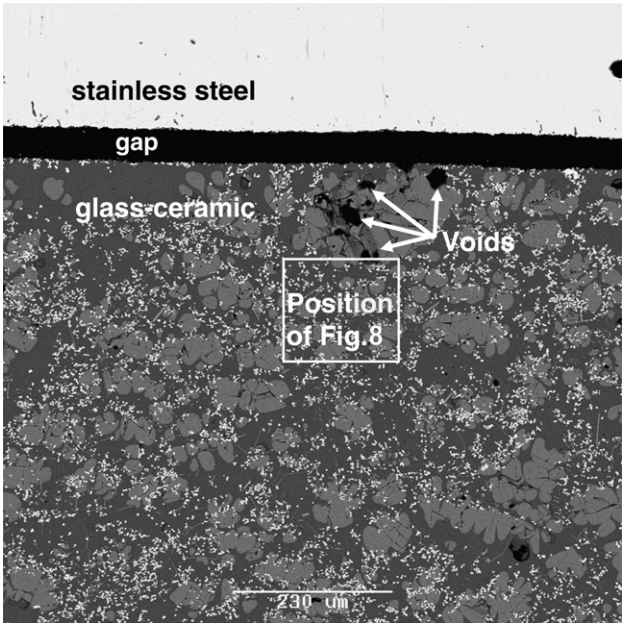

Fig. 6. SEM backscattered electron micrograph of the interface between the SS can and the glass–ceramic. Note gap produced during sample preparation (cutting and mounting) due to low adhesion of the glass–ceramic to the SS can. See Fig. 2 for microstructural detail within the glass–ceramic.

presence of such a Cr-rich phase at depth in the glass implies that Cr mobility and solubility in the glass are the main features in the SS/glass interactions.

The Cr concentration at the glass side of the interface is about 1.5 wt% and declines sharply after 100 μm to the value for the pure glass matrix (traversing from the interface into the waste form, avoiding any crystalline phases), which is consistent with the depth at which the acicular Cr-rich phase mentioned above is observed. Fe concentrations do not vary greatly, generally within the EDS analysis errors.

3.4. Comparison with SS/synroc interactions

Previous studies indicated that the interactions between SS and synroc (titanate ceramics) under HIPing conditions (1280 °C/100 MPa) resulted in the formation of a complex multi-layered reaction region (~300 μm thick) [9]. Fe^{2+} diffusion in the ceramics dominated the interactions and imposed minor changes on the microstructure of the titanate phases near the interface. In contrast to the SS/synroc interactions, the interactions between SS and glass in this work are mainly controlled by Cr diffusion and solubility in the glass matrix.

3.5. Characterisation of the surface of the specimens after leaching

The whole HIPed specimen and the tabular sub-specimens after leaching showed slight surface alteration, exhib-

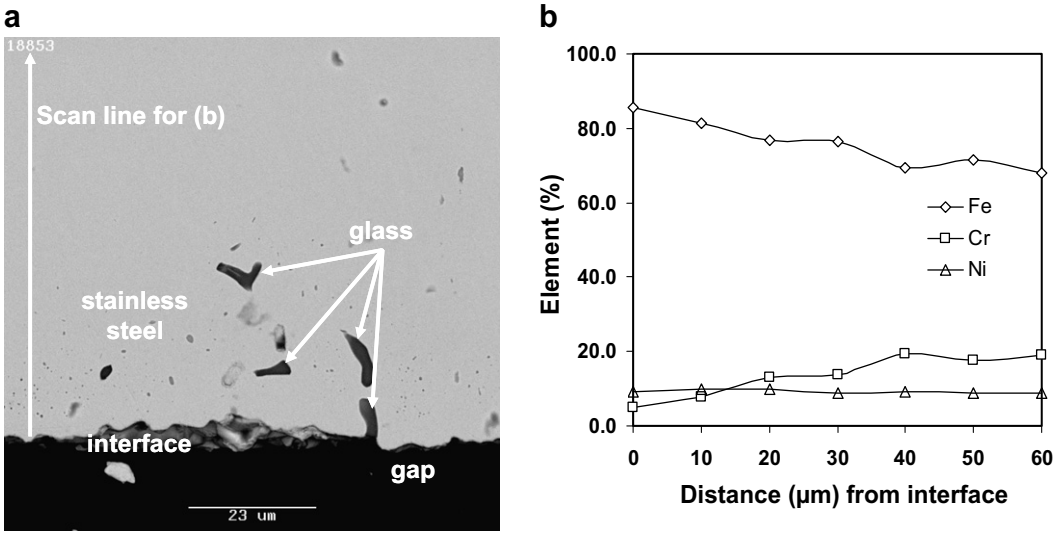

Fig. 7. SEM backscattered electron micrograph of the SS component of the interface (a) showing glass penetrations into the SS can wall, and elemental profiles of Fe, Cr and Ni as a function of distance (μm) away from the interface into the can wall (b).

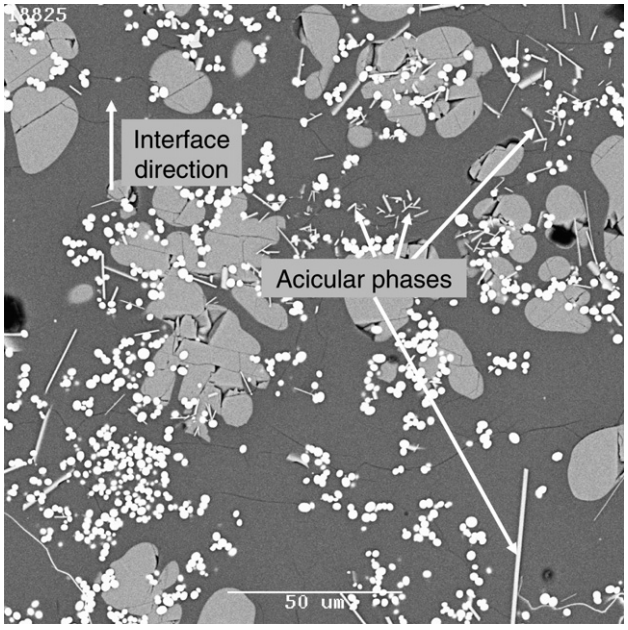

Fig. 8. SEM backscattered electron micrograph showing the formation of a crystalline acicular phase rich in Cr and Al oxide in the glass–ceramic at 200–400 μm depth from the interface. The position is marked in Fig. 6. Other phases are as in Fig. 2.

ited in the first instance by a change in colour, as a result of leaching in deionised water at 90 °C for 56 days.

SEM backscattered electron micrographs of the tabular sub-specimens before and after leaching (see Fig. 9) clearly showed a distinct surface alteration after leaching. The surface roughness does not conceal the degradation of the surface as a result of leaching, where the glassy matrix has dissolved leaving the more leach-resilient crystalline constituents, particularly zirconia (small round particles), effectively protruding from the surface. The extent of fluorite dissolution is not clear. There is evidence of grain boundary dissolution around most of the fluorite grains; however, this is most likely from the dissolution of the surrounding glassy matrix, similar to the zirconia grains.

Cross-sectional SEM backscattered electron micrographs of the tabular sub-specimens before and after leaching (see in Fig. 10) confirmed that leaching of the sub-specimen in deionised water at 90 °C for 56 days created an alteration layer ~30 μm on the leached surface and the dissolution of glass matrix along the fluorite grain boundaries is the main feature for this glass–ceramic leached in deionised water. Further SEM–EDS analysis did not reveal any preferential releases of Na/Ca from the surface alteration layer.

3.6. Effect of SS/glass–ceramic interactions on the chemical durability of the waste form

The normalised leach rates for the tabular sub-specimens (representing the non-affected zone distal to the interaction layer) and for the whole HIPed specimen (with the interaction zone present) are given in Figs. 11 and 12, respectively. The estimated errors on these elemental release rates vary largely with elements, ranging from 0.3% to 10%. In general, elemental releases decrease with time, by about an order of magnitude over the 56 days, with most elemental releases for the final two leach periods being similar, ranging from 0.1 to 1 g m^{-2} day^{-1}.

The dissolution of the tabular sub-specimens is not congruent (see Fig. 11) with relatively lower F (an order of magnitude lower), Ca (a factor of 2–3 lower) and Zr (nearly four orders of magnitude lower, not shown in Fig. 11) releases than those of the other matrix elements, which is consistent to the SEM observations with dissolution of glass along CaF_2 grain boundaries leaving ZrO_2 protruding from the leached surface. A comparison of elemental releases between the tabular sub-specimen and the whole

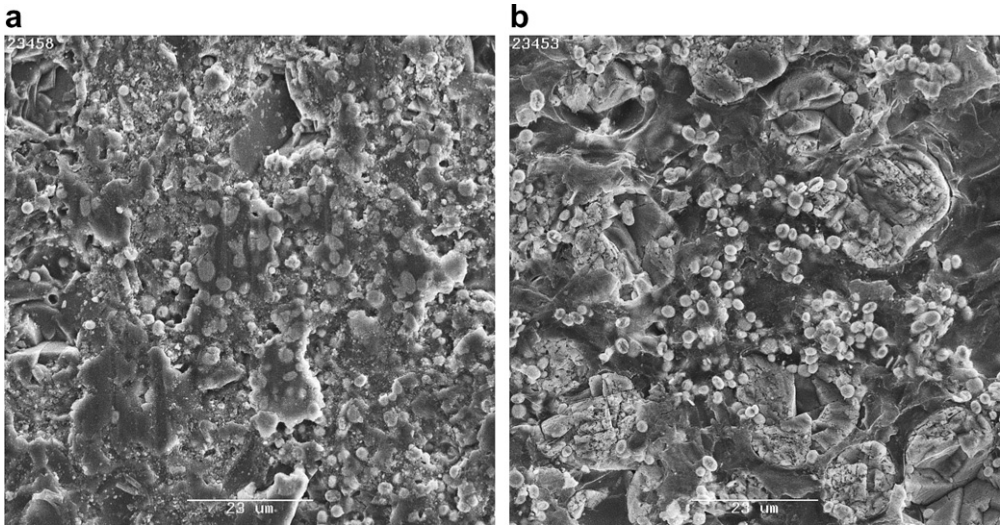

Fig. 9. SEM backscattered electron micrographs of the tabular sub-specimen surface before (a) and after (b) leaching in deionised water at 90 °C for 56 days. There is clearly degradation of the surface of the leached sub-specimen insofar as ZrO_2 particles protruding from the leached surface.

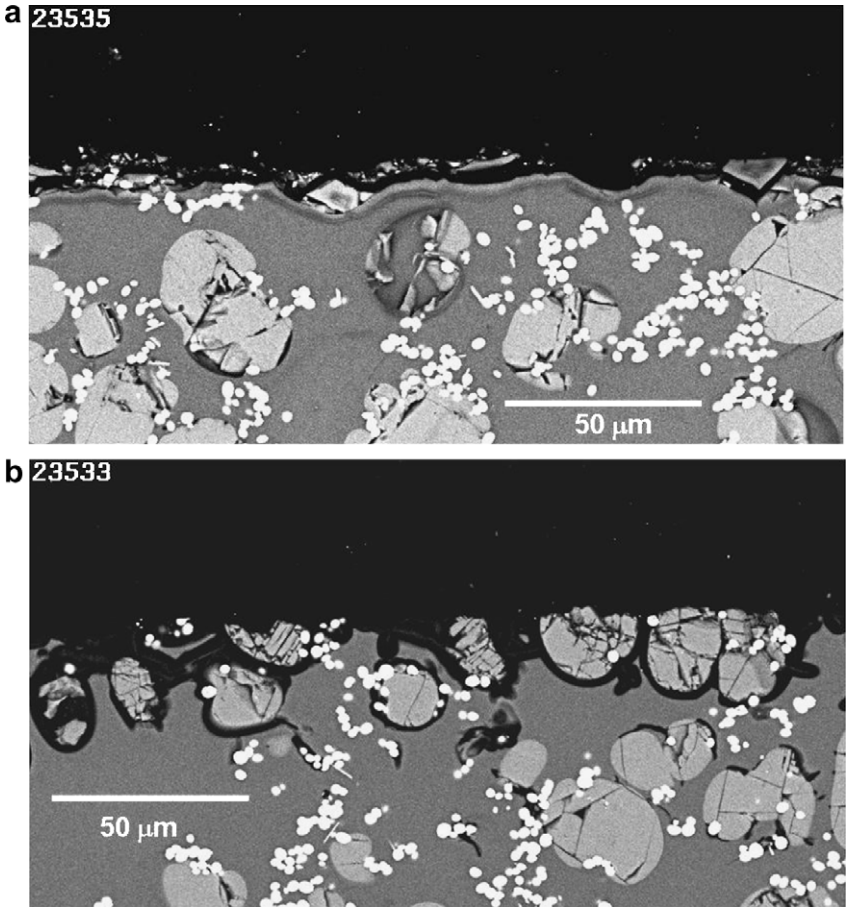

Fig. 10. Cross-section SEM backscattered micrographs of the tabular sub-specimen surface before (a) and after (b) leaching in deionised water at 90 °C for 56 days.

HIPed specimen show that they are similar for all elements, for each time interval, except for slightly elevated releases of Cr and Mo from the whole HIPed specimen.

The leach testing in deionised water at 90 °C confirmed that the SS/glass–ceramic interactions did not have any notable negative effects on the chemical durability of the

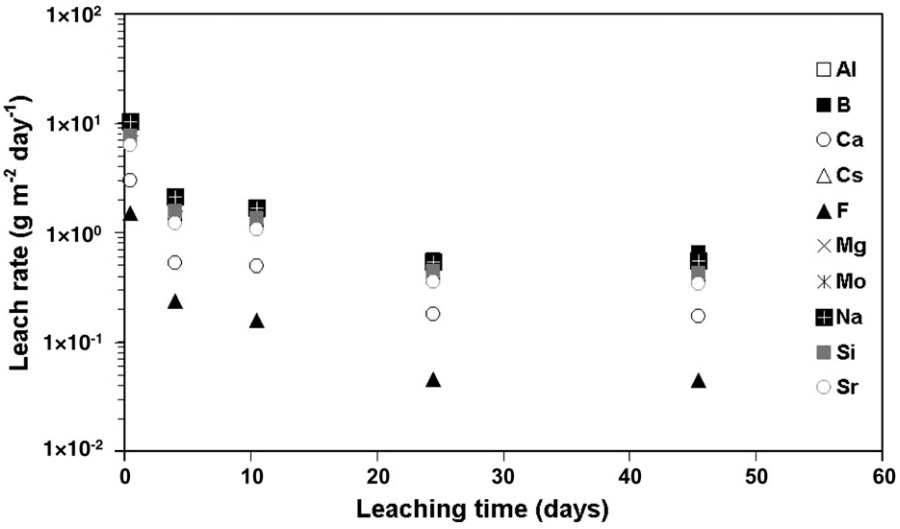

Fig. 11. Normalised mean leach rates of the tabular sub-specimens leached in deionised water at 90 °C for up to 56 days (midpoints of leaching periods were used in the plot).

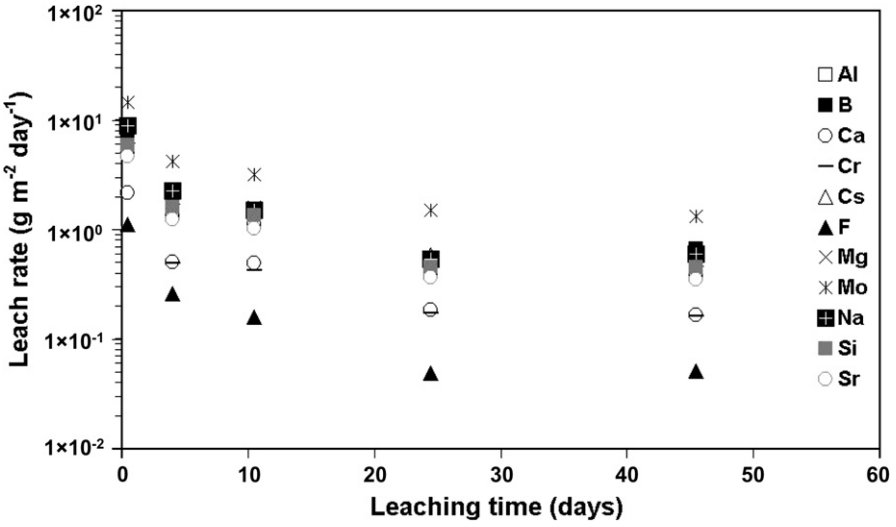

Fig. 12. Normalised mean leach rates of the whole HIPed specimen leached in deionised water at 90 °C for up to 56 days (midpoints of leaching periods were used in the plot).

glass–ceramic as a waste form. The elevated Cr and Mo levels in the leachates from the whole HIPed specimen are attributed to the higher levels of accessible Cr and Mo in the interaction layer on the outermost of the waste form.

For the glass–ceramic remote from the SS/waste form interface, the relatively lower F and Ca releases suggest that crystalline fluorite (CaF_2) is relatively more durable than the glassy matrix at the test conditions. In all cases, Zr releases are either undetectable or about three orders of magnitude lower than those of the glassy matrix, suggesting its primary association with the more durable zirconia in the waste form. These findings are consistent with the SEM results where the leached specimens showed that the glassy matrix has been more substantially attacked during leaching than the crystalline components, zirconia and fluorite.

4. Conclusions

HIPing under an argon atmosphere resulted in the formation of a thin (up to 3 μm) layer of Cr_2O_3 and Fe_3O_4 on the outer surface of the 304 SS can. The reaction of SS and the glass–ceramic did not have any significant effect on either the glass or ceramic phases near the interface, with only subtle Cr depletion at the inner surface of the SS can (~40 μm thick). The presence of a crystalline acicular Cr-rich phase at 200–400 μm depth in the glass–ceramic indicates that Cr mobility and solubility in glass dominate the SS/glass–ceramic interactions. Overall, the SS/glass–ceramic interactions under HIPing conditions have no significant impact on the SS cans and do not produce any undesirable phases that would have a detrimental effect on the chemical durability of the glass–ceramic waste form.

Acknowledgements

We are grateful to S. Moricca, T. Eddowes and N. Webb for HIPing, G. Smith for sample preparation, K. Short for assistance with X-ray diffraction, R.A. Day for glass–ceramic formulation and E.R. Vance for comment and discussions.

References

[1] M.D. Staiger, Calcine Waste Storage at the Idaho Nuclear Technology and Engineering Center, INEEL/EXT-98-00455, 1999.
[2] B.D. Begg, R.A. Day, S. Moricca, M.W.A. Stewart, E.R. Vance, in: Paper Presented at Waste Management, 27 February–3 March, Tucson, AZ, USA, 2005.
[3] R.A. Day, J. Ferenczy, E. Drabarek, T. Advocat, C. Fillet, J. Lacombe, C. Ladirat, C. Veyer, R. Do Quang, J. Thomasson, in: WM'03 conference, 23–27 February, Tucson, AZ, USA, 2003.
[4] G.R. Lumpkin, K.L. Smith, M.G. Blackford, R. Giere, C.T. Williams, Micron 25 (6) (1994) 581.
[5] ASTM C 1220-98, Standard Test Method for Static Leaching of Monolithic Waste Forms for Disposal of Radioactive Waste, ASTM International, 1998.
[6] M. Ghoranneviss, A. Shokouhy, S.H. Haji Hosseini Grazesatni, A.H. Sari, M.R. Hantehzadeh, in: XXVIIth ICPIG, Eindhoven, Netherlands, 18–22 July, 2005.
[7] K. Tsukimura, S. Sasaki, N. Kimizuka, Jpn. J. Appl. Phys., Part 1 36 (1997) 3609.
[8] W. Sitte, Mater. Sci. Monogr. A (React. Solids, Pt. A) 28 (1985) 451.
[9] H. Li, Y. Zhang, P.J. McGlinn, S. Moricca, B.D. Begg, E.R. Vance, J. Nucl. Mater. 355 (2006) 136.